Magnetically levitated autoparametric broadband vibration energy harvesting

L. Kurmann[1], Y. Jia[2], Y. Manoli[3] and P. Woias[3]

[1]University of Applied Sciences and Arts Northwestern Switzerland, Switzerland
[2]Department of Mechanical Engineering, Thornton Science Park, University of Chester, UK
[3]Department of Microsystems Engineering, IMTEK, University of Freiburg, Germany

E-mail: lukas.kurmann@fhnw.ch; yu.jia.gb@ieee.org

Abstract. Some of the lingering challenges within the current paradigm of vibration energy harvesting (VEH) involve narrow operational frequency range and the inevitable non-resonant response from broadband noise excitations. Such VEHs are only suitable for limited applications with fixed sinusoidal vibration, and fail to capture a large spectrum of the real world vibration. Various arraying designs, frequency tuning schemes and nonlinear vibratory approaches have only yielded modest enhancements. To fundamentally address this, the paper proposes and explores the potentials in using highly nonlinear magnetic spring force to activate an autoparametric oscillator, in order to realize an inherently broadband resonant system. Analytical and numerical modelling illustrate that high spring nonlinearity derived from magnetic levitation helps to promote the 2:1 internal frequency matching required to activate parametric resonance. At the right internal parameters, the resulting system can intrinsically exhibit semi-resonant response regardless of the bandwidth of the input vibration, including broadband white noise excitation.

1. Introduction

The mainstream of vibration energy harvesting (VEH) has often relied on oscillators operating in direct resonance in order to accumulate mechanical energy [1]. Such an approach leads to a system that only exhibits resonant response within a specific bandwidth of excitation frequencies. By adjusting the quality factor, widening of this bandwidth would inevitably sacrifice the power peak. Various frequency tuning and frequency broadening strategies have been extensively investigated [2], however, the enhancements to date are still relatively modest and proposed systems are still confined to a particular operational frequency range.

Arraying of either coupled or uncoupled oscillators with varying resonant frequencies can help to accumulate to a relatively wide frequency range, though the power density of the overall system compares unfavorable to a single large oscillator that takes up the whole volume [3]. A multitude of frequency tuning mechanisms, either mechanical or electrical, typically require power input; therefore, it is still limited to single frequency sources that only require intermittent tuning [4]. Duffing nonlinearity has been extensively explored [2, 3], but bandwidth broadening is modest and proposed enhancements towards noise excitations are disputable [5].

Parametric resonance on the other hand is a fundamentally different nonlinear vibratory phenomenon [6] invoked through Mathieu instability and has the potential to exhibit nonlinear broadband behavior [7]. Parametrically excited VEH has been previously demonstrated

enhancements in both power peak and the frequency bandwidth [8] over conventional direct resonant VEH. Furthermore, unlike direct resonance, it is possible to simultaneously enhance both power peak and frequency bandwidth with lower damping [9]. However, its activation is non-trivial due to stringent stability bounds and initiation amplitude thresholds [10].

One design route is to establish an autoparametric system where external direct excitation is internally coupled to parametric excitation through a strict 2:1 internal frequency ratio. This has been numerically and experimentally validated [11] with a coupled two degrees of freedom (DOF) oscillatory system at its most basic form, yielding substantially more favorable results than a direct oscillator. Furthermore, the use of strong spring nonlinearity in the first DOF has been suggested as a means to more readily access Mathieu instability [12], while the use of magnetic spring through magnetic levitation [13] is a potential source of intrinsic nonlinearity.

2. Method

2.1. Design

The proposed design (figure 1) consisting of a pair of magnets carrying a pendulum oscillator is magnetically levitated between repulsive magnetic fields from both top and bottom. Figure 2 illustrates the system model where external excitation is directly applied to a strongly nonlinear magnetic spring, which is in turn coupled to the secondary pendulum oscillator.

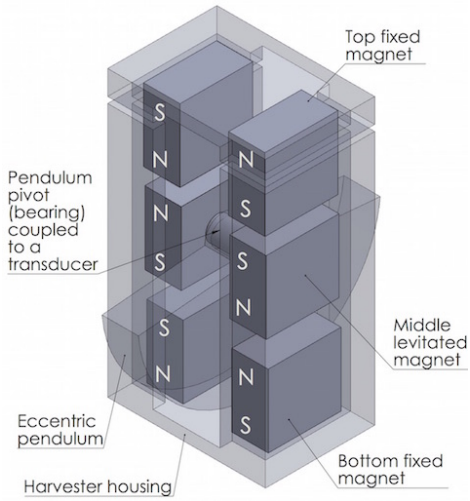

Figure 1. Design of the system with three opposite directed permanent magnet pairs.

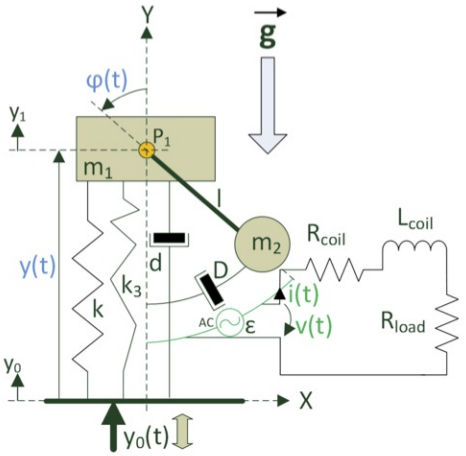

Figure 2. Lumped parameter model with attached transducer shown on the right hand side. k and k_3 are linear and nonlinear springs.

2.2. Model

While magnetic spring restoring force is often reduced to a simple cubic Duffing type nonlinearity added to a linear spring term [13], a more complicated polynomial expression term can be derived from the magnetic dipole interactions [14] as shown in in equation 1.

$$F(t) = -\frac{6\mu_0 M^2}{\pi(r-|y|)^5} y \tag{1}$$

where, r is the total spacing between the magnets at zero displacement, y is the vertical displacement of the magnetically levitated mass, $(r-y)$ is thus the spacing between the magnet dipoles, M is the dipole moment and μ_0 is the relative permeability. Figure 3 compares the restoring force derived from these two approaches as well as a linear spring force. It can be

noted that the Duffing approximation holds for small displacements. Therefore, the governing equation of the primary oscillator alone can be approximated by equation 2.

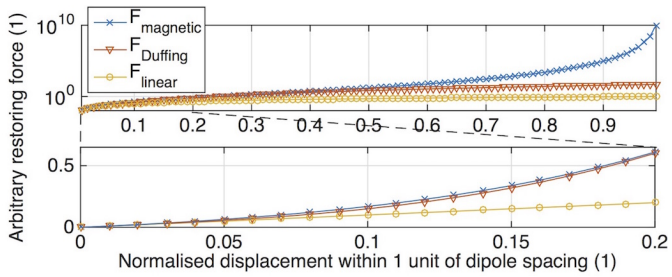

Figure 3. Comparing spring restoring force described by dipole interaction, Duffing nonlinearity and linear spring. Bottom plot is the zoom of the top plot.

$$\ddot{y} + 2\zeta\Omega_0\dot{y} + \Omega_0^2 y + \beta y^3 = A_y\omega^2\cos(\omega t) \tag{2}$$

where, ζ is the damping ratio for this primary oscillator in the y axis, Ω_0 is the natural frequency for this primary oscillator, β is the Duffing coefficient, A_y is the excitation displacement amplitude in the vertical direction, ω is the excitation frequency and t is the time domain.

The response $y(t)$ feeds into the pendulum oscillator, of which the response can thus be modelled by equation 3 (for direct oscillations) and/or equation 4 (for parametric oscillations).

$$\ddot{\varphi} + \gamma\dot{\varphi} + \omega_0^2\sin\varphi = \frac{A_x}{l}\omega^2\cos(\omega t)\cos\varphi \tag{3}$$

$$\ddot{\varphi} + \gamma\dot{\varphi} + \xi\dot{\varphi}|\dot{\varphi}| + [\omega_0^2 - \frac{\ddot{y}(t)}{l}]\sin\varphi = 0 \tag{4}$$

where, φ is the angular displacement of the pendulum, γ is the viscous damping coefficient, ξ is nonlinear damping coefficient, ω_0 is the natural frequency of the pendulum, l is the effective pendulum length and A_x is the horizontal excitation displacement where applicable.

With the onset of parametric resonance in the subsidiary pendulum oscillator, the resulting unidirectional flow of energy limits the oscillatory amplitude growth of the primary levitated oscillator. This is described with the inclusion of a mode coupling term ψ [11] in equation 5.

$$\ddot{y} + 2\zeta\Omega_0\dot{y} + \Omega_0^2 y + \beta y^3 - \psi[\cos(\varphi)\dot{\varphi}^2 + \sin(\varphi)\ddot{\varphi}] = A_y\omega^2\cos(\omega t) \tag{5}$$

Extensive numerical simulations in MATLAB were carried out to better understand the derived systems. The ODE45 Dormand-Prince solver was employed.

3. Results and Discussion

3.1. Spring nonlinearity and frequency response

The internal frequency ratio of the 2-DOF system was matched to 2:1. However, the presence of the displacement-dependent nonlinearity results in the modulation of this ratio during vibration (figure 4), thus promoting the chance of operating around the 2:1 frequency ratio even if for slightly detuned scenarios (figure 5) common as a result of manufacturing tolerance.

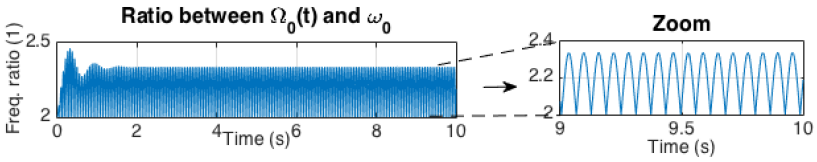

Figure 4. Modulation of internal frequency ratio during oscillation.

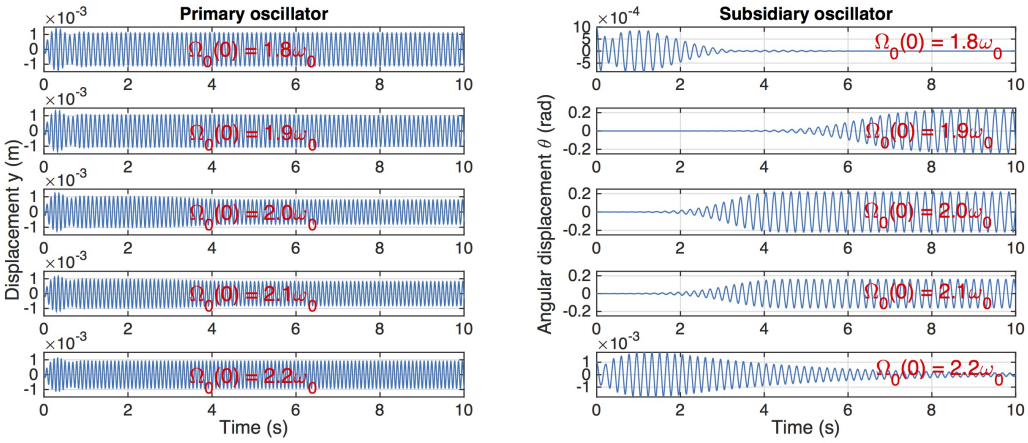

Figure 5. The activation of parametric resonance for varying initial internal frequency ratios.

Figure 6 presents the frequency domain characteristics of the two coupled oscillators for a given acceleration. In addition to the typical spring hardening peak bending for the primary oscillator, there is also a dip where energy is pumped to the secondary oscillator as parametric resonance onsets; thus, creating two peaks for the same resonant regime. The normalised −3dB bandwidth (shaded region) of the directly excited primary oscillator is 0.134, in contrast to 0.195 (∼45% enhancement) of the parametrically excited secondary oscillator. However, a sine wave frequency sweep does not reveal the full frequency responsiveness of the autoparametric system.

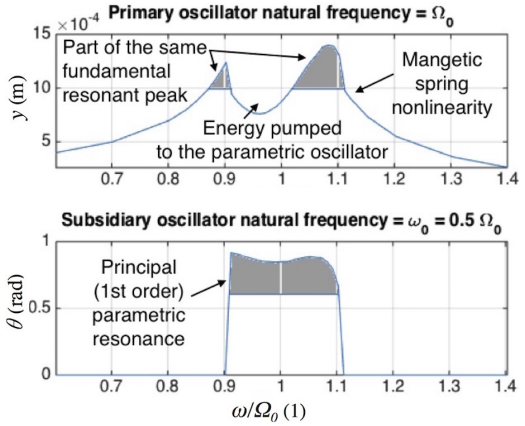

Figure 6. Frequency domain response of directly excited primary oscillator and parametrically excited oscillator.

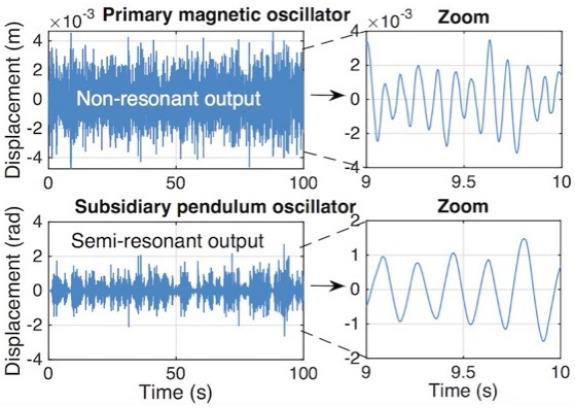

Figure 7. Time domain response when subjected to band-limited (0 Hz - 1 kHz) white noise vibration.

3.2. Noise response

When subjected to noise excitation, the primary magnetic oscillator exhibits non-resonant impact-induced output, which rapidly decays away at around its natural frequency. This is then internally coupled through the 2:1 frequency ratio to parametrically activate semi-resonant response as shown in figure 7. The semi-resonant response can be seen across varying bandwidth as illustrated with 100 Hz band-limited noise (figure 8) and 1 kHz band-limited noise (figure 9).

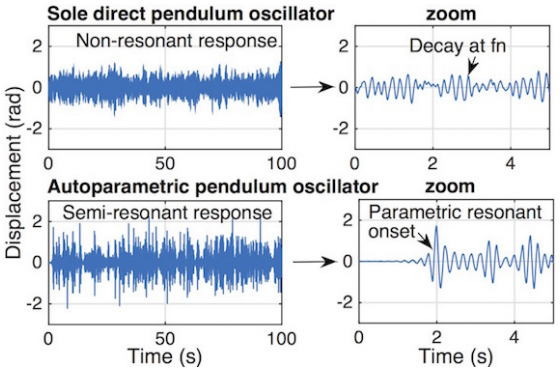

Figure 8. Response from band-limited (0 Hz -100 Hz) white noise at 6.6×10^4 g^2/Hz.

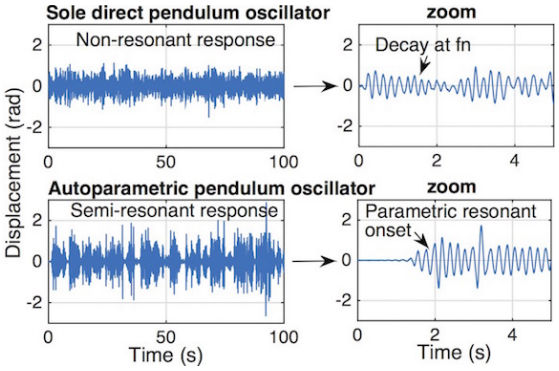

Figure 9. Response from band-limited (0 Hz - 1 kHz) white noise at 6.6×10^4 g^2/Hz.

Figure 10 compares the proposed system with a comparable directly excited pendulum oscillator under broadband noise excitation. It shows that beyond a certain noise threshold, the autoparametric system increasingly performs better than its direct counterpart due to its inherent ability to attain semi-resonant. This gap further widens at higher noise levels.

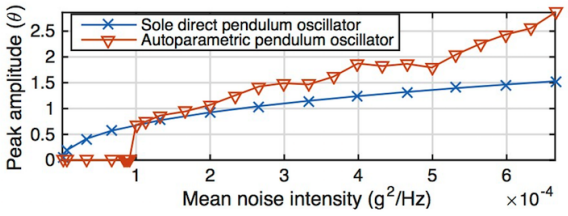

Figure 10. Peak amplitude of the proposed auto-parametric system (semi-resonant output) compared to a conventional direct oscillator when subjected to band-limited (0 Hz - 1 kHz) white noise.

4. Conclusion

This paper explored a pathway towards a highly nonlinear autoparametric VEH solution that has broader operational frequency bandwidth than linear direct oscillators and can inherently exhibit semi-resonant response under broadband noise excitations. The harvester solution would thus be suitable for capturing a broad range of vibration sources. Future work involves experimental investigation, incorporation of transduction mechanisms, and validation with various measured vibration profiles from various applications.

References

[1] S.P. Beeby, M.J. Tudor and N.M. White, 2006, *Meas. Sci. Technol.*, **17**, R175-R195
[2] D. Zhu, M.J. Tudor and S.P. Beeby, 2010, *Meas. Sci. Technol.*, **21**, 29pp
[3] L. Tang, Y. Yang C.K. Soh, 2010, *J. Intel. Mater. Syst. Struct.*, **21**(18), pp. 1867-97
[4] D. Zhu, S. Roberts, M.J. Tudor and S.P. Beeby, 2010, *Sens. Actuators A*, **158**(2), pp. 284-293
[5] R.S. Langley, 2015, *J. Sound Vib.*, **339**, pp. 247-61
[6] A. Nayfeh and D. Mook, *Nonlinear Oscillation*, (Wiley, 1979)
[7] L. Kurmann *et al.*, 2015, *J. Phys. Conf. Ser.*, **660**(1), p 012070
[8] Y. Jia, J. Yan, K. Soga and A.A. Seshia, 2014, *J. Intel. Mater. Syst. Str.*, **25**(3), pp 278-89
[9] Y. Jia, J. Yan, K. Soga and A.A. Seshia, 2013, *J. Phys. Conf. Ser.*, **476**(1), p 012126
[10] Y. Jia, J. Yan, K. Soga and A.A. Seshia, 2014, *Smart Mater. Struct.*, **23**(6), p 065011
[11] Y. Jia, J. Yan, K. Soga and A.A. Seshia, 2014, *Sens. Actuators A*, **220**, pp 69-75
[12] B. Vazquez-Gonzalez and G. Silva-Navarro, 2008, *Shock Vibration*, **15**(3-4), pp 355-68
[13] B. P. Mann, N. D. Sims, 2009, *J. Sound Vib.*, **319**(1-2), pp. 515?30
[14] K. W. Yung, P. B. Landecker, and D. D. Villani, 1998, *Mag. Elect. Sep.*, **9**(1), pp 39?52